Synthesis and Analysis of a Novel Linkage Mechanism with the Helical Motion of the End-Effector

Alexey Fomin [1,*] **, Daniil Petelin** [1] **and Andreas Jahr** [2]

[1]   Mechanisms Theory and Machines Structure Laboratory, Mechanical Engineering Research Institute of the Russian Academy of Sciences (IMASH RAN), Moscow 101990, Russia; petelin_daniil@inbox.ru

[2]   Faculty of Mechanical and Process Engineering, Düsseldorf University of Applied Sciences, 40476 Düsseldorf, Germany; andreas.jahr@hs-duesseldorf.de

*   Correspondence: alexey-nvkz@mail.ru

check for updates

Abstract: The proposed study is focused on the development of a novel modification of the slider-crank mechanism, the kinematic scheme of which is organized by coupling planar and spatial (screw) kinematic chains. The structure of this mechanism provides the end-effector with a cyclic movement along a helicoidal trajectory, while all other links have planar motions. A kinematic analysis of the synthesized mechanism is discussed in this study. The motion variables of the end-effector at different pitches in the screw joints are determined analytically and numerically. Based on the mechanism's kinematic scheme, its assembling computer-aided design (CAD) model has been created, in accordance with which a physical prototype has been built. A functional performance of the prototype is studied by comparing the displacements of its end-effector with analogical displacements of the CAD model. The question of the technological application of the developed mechanism for spring winding and various objects' screwing has been considered in this study.

Keywords: slider-crank mechanism; screw mechanism; degree-of-freedom; Assur group; trajectory

1. Introduction

Improvement of the machine-building industry is directly related to the development of new mechanisms and machines. Their efficiency and functional properties largely depend on the kinematic schemes on the basis of which they are designed. Structural synthesis, which is one of the basic subdisciplines of mechanisms and machines science (MMS), not only allows for creating fundamentally novel mechanical systems but also ensuring their efficiency already at the stage of designing their kinematic schemes. There are various methods and algorithms for structural synthesis, including those methods that are based on graph theory [1,2], on the use of closed multi-degree-of-freedom (DoF) kinematic chains [3], on screw theory [4,5], on the application of mobility formulas [6,7]. The method of sequential coupling of kinematic chains (structural groups) with zero DoF is quite widely used [8]. This method had been firstly proposed by Assur L.V. and formulated by him for planar mechanisms. In these mechanisms, all coupled zero DoF kinematic chains (Assur groups) are placed in one or several parallel planes. This principle is kept both for mechanisms with sequential structure and for parallel mechanisms [9–11]. In [12], a related approach is demonstrated for developing complex screw mechanisms.

However, the coupling of exclusively planar kinematic chains, including chains with zero DoF, is quite particular case in mechanisms synthesis. Due to the fact that kinematic chains can be designed with different types of imposed constraints, various cases of their coupling are possible. For example, planar kinematic chains can also be coupled with spherical or wedge chains that have three imposed constraints like planar chains, but the type of these constraints is different [13]. The main criterion for

such a coupling is the coincidence of the movements of combined kinematic chains. In the absence of even one common movement, the joint functioning of these chains in one mechanism cannot be realized. Such a case is, for example, the combination of a spherical chain having rotations of links around each coordinate axis and a wedge chain having translational displacements of links along each coordinate axes. Because these kinematic chains lack any common movement, it is impossible to achieve their joint functioning in one mechanism.

At the same time, mechanisms that include different types of kinematic chains allow implementing fundamentally new motion laws and performing novel technological operations. Such mechanisms have all the design advantages of kinematic chains on the basis of which they are constructed. This study aims to develop and analyze a novel mechanism, which simultaneously includes planar and spatial kinematic chains. In this case, the condition of assuring the minimum number of links, kinematic pairs and drives while having spatial movement of an end-effector in the synthesized mechanism is made.

This paper is organized as follows. Section 2 provides structural synthesis and analysis of the developed linkage mechanism in terms of kinematic chains included in its composition. Section 3 presents an analytical solution of kinematics of the synthesized mechanism. Section 4 shows a numerical calculation of the kinematic parameters when setting different pitches in screw joints. Section 5 considers the creation of a CAD model of the synthesized mechanism and fabrication of its physical prototype. Section 6 presents possible practical applications when performing specific technological operations. Conclusions are discussed in Section 7.

2. Structural Synthesis and Analysis of the Mechanism

Address to the development of the proposed linkage mechanism and specify the synthesis conditions in the following formulation:

- Provide a single drive in the mechanism (i.e., provide mobility one, $W = 1$) and reproducing the spatial cyclic motion of the end-effector. Accept screw motion as the output motion, in which simultaneous rotation and translational displacements are realized;
- Provide the minimum number of links and kinematic pairs in the mechanism. Accept the condition that each link will be double-paired, i.e., forming only two kinematic pairs with the other links. Accept only one-DoF joints, providing speedwork and reliability when transmitting movements among links of the mechanism;
- Provide the position of maximum number of movable links of the mechanism in one or several parallel planes to minimize dynamic loads during its operation.

Determine structural parameters for planar and spatial kinematic chains according to the synthesis conditions. For the planar kinematic chain, these parameters can be found from the following mobility formula

$$W = 3n - 2p_5 - p_4, \tag{1}$$

where W is the mobility of a kinematic chain, defining the number of its DoF; n is the number of movable links; p_5 and p_4 are the numbers of one- and two-DoF kinematic pairs.

Accepting $W = 0$ (necessary criterion for a kinematic chain with zero DoF) and using only one-DoF joints, the simplest solution from (1) is $n = 2$, $p_5 = 3$ and $p_4 = 0$. Take dyad *RRP* as a planar kinematic chain based on the obtained solution.

Chose helical kinematic chain as a spatial one because it could be created with minimum number of links and includes only one-DoF joints. The structure of screw kinematic chains is described by the following mobility formula

$$W = 2n - p_5, \tag{2}$$

from which, with $W = 0$, the simplest solution is $n = 1$ and $p_5 = 2$. This condition corresponds to a one-bar kinematic chain (monade). Thus, governing Equations (1) and (2) allow defining structural

parameters for targeted kinematic chains, including zero DoF chains when $W = 0$ or mechanisms with various DoFs when W possesses values of positive integers.

Further, sequentially couple with the driving link dyad *RRP*, and then screw monade. The position of screw monade in the mechanism is provided in such a way that its translational displacement coincides with the translational displacement of dyad *RRP*. The mechanism designed in this way is shown in Figure 1a. Here, 1—crank (driving link), 2—connecting rod, 3—slider, 4—nut (end-effector), 5—fixed link, 6—function element integrated with nut 4. Kinematic pairs 5-1, 1-2 and 2-3 are rotational with parallel axes. Kinematic pair 3-5 is prismatic. Kinematic pairs 3-4 and 4-5 are screw. Figure 1b shows the elements of screw part of the synthesized mechanism where pitch p_1 is in pair 3-4 and pitch p_2 is in pair 4-5.

(**a**)   (**b**)
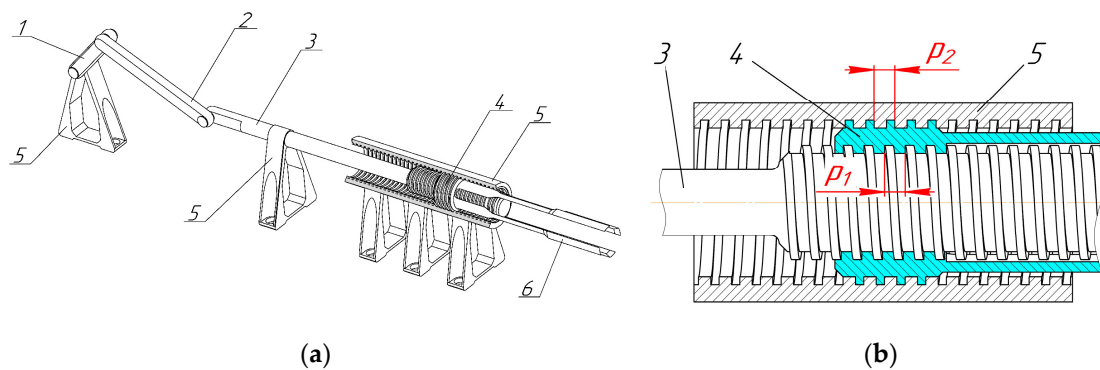
Figure 1. (**a**) Synthesized linkage mechanism: 1-driving link (crank); 2 and 3-connecting rod and slider forming dyad *RRP* with zero DoF; 4-end-effector (nut) forming screw monade with zero DoF; 5-fixed link; 6-function element rigidly integrated with nut 4; (**b**) screw part of the mechanism having helical joints 3–4 and 4–5.

The input movement is given to crank 1 and transmitted through connecting rod 2 to slider 3, which forces end-effector 4 to reproduce an output helical movement. A specific constructive condition in the mechanism is in providing non-self-braking of its links in kinematic pairs 3-4 and 4-5, when the helix angle (ψ) must be greater than the reduced friction angle (μ), i.e., $\psi > \mu$, where $\psi = arctg(p \cdot k / \pi \cdot d)$, p is the thread pitch, k is the number of starts in the screw part, d is the diameter of screw link, $\mu = arctg(f_F)$, f_F is the superficial friction factor in thread, $f_F = f / cos(\gamma)$, f is the friction coefficient, γ is the tilt angle of a thread flank.
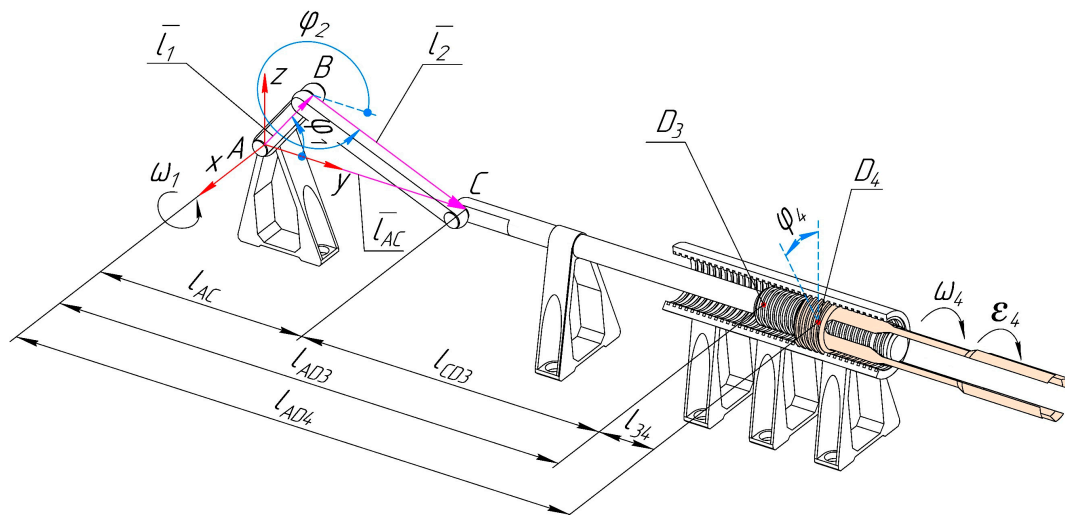
3. Kinematic Analysis of the Mechanism

Address to the kinematics analysis of the synthesized linkage mechanism. There are different methods of kinematic analysis of mechanisms having screw joints [14–16]. Present the crank-slider part of the synthesized mechanism as closed contour *ABCA* (Figure 2), described by the vector sum:

$$\overline{l_1} + \overline{l_2} - \overline{l_{AC}} = 0. \tag{3}$$

Projecting vector Equation (3) on axes y and z obtains:

$$\begin{cases} l_1 cos\varphi_1 + l_2 cos\varphi_2 = l_{AC}; \\ l_1 sin\varphi_1 + l_2 sin\varphi_2 = 0, \end{cases} \tag{4}$$

where l_1 is the length of crank 1, l_2 is the length of connecting rod 2, φ_1 is the rotational angle of crank 1, φ_2 is the rotational angle of connecting rod 2.

Figure 2. Toward kinematic analysis of the synthesized linkage mechanism.

Express φ_2 from the second Equation of system (4) in the following view:

$$\varphi_2 = -arcsin\left(\frac{l_1 sin\varphi_1}{l_2}\right). \tag{5}$$

Variable length l_{AC} can be found from the first Equation of system (4) with consideration of Equation (5) as:

$$l_{AC} = l_1 cos\varphi_1 + l_2 cos\left(arcsin\left(\frac{l_1 sin\varphi_1}{l_2}\right)\right). \tag{6}$$

Define expressions for determining linear velocity of point C (V_C) and angular velocity of connecting rod 2 (w_2) by differentiating the Equations of system (4) with respect to generalized coordinate φ_1:

$$\begin{cases} -l_1 sin\varphi_1 - u_{21} l_2 sin\varphi_2 = V_{C\varphi1}; \\ l_1 cos\varphi_1 + u_{21} l_2 cos\varphi_2 = 0, \end{cases} \tag{7}$$

where $V_{C\varphi1} = dl_{AC}/d\varphi_1$ and $u_{21} = d\varphi_2/d\varphi_1$ are the analogs of linear and angular velocities.

Express parameter u_{21} from the second Equation of system (7) as:

$$u_{21} = -(l_1 cos\varphi_1)/(l_2 cos\varphi_2) \tag{8}$$

and, introducing it into the first Equation of system (7), express the analog of linear velocity ($V_{C\varphi1}$) as:

$$V_{C\varphi1} = l_1(cos\varphi_1 tg\varphi_2 - sin\varphi_1). \tag{9}$$

The true values of linear velocity of point C (V_C) and angular velocity of connecting rod 2 (w_2) can be determined as:

$$V_C = w_1 V_{C\varphi1}, \ w_2 = w_1 u_{21}. \tag{10}$$

Then, find linear acceleration of point C (a_C) and angular acceleration of connecting rod 2 (ε_2) by differentiating the Equations of system (7) by generalized coordinate φ_1:

$$\begin{cases} -l_1 cos\varphi_1 - u_{21}^2 l_2 cos\varphi_2 - u_{21}' l_2 sin\varphi_2 = a_{C\varphi1}; \\ -l_1 sin\varphi_1 - u_{21}^2 l_2 sin\varphi_2 + u_{21}' l_2 cos\varphi_2 = 0, \end{cases} \tag{11}$$

where $a_{C\varphi1} = dV_{C\varphi1}/d\varphi_1$ and $u_{21}' = du_{21}/d\varphi_1$ are the analogs of linear and angular accelerations.

Express parameter u'_{21} from the second Equation of system (11) as:

$$u'_{21} = \frac{l_1}{l_2 cos\varphi_2}\left(sin\varphi_1 + \frac{l_1 cos^2\varphi_1 sin\varphi_2}{l_2 cos^2\varphi_2}\right), \qquad (12)$$

and introduce it into the first Equation of system (11) and then express parameter $a_{C\varphi1}$ as:

$$a_{C\varphi1} = -l_1(cos\varphi_1 + sin\varphi_1 tg\varphi_2) - \frac{l_1^2 cos^2\varphi_1}{l_2 cos^3\varphi_2}. \qquad (13)$$

The true values of linear acceleration of point C (a_C) and angular acceleration of connecting rod 2 (ε_2) are determined as:

$$a_C = w_1^2 a_{C\varphi1} + \varepsilon_1 V_{C\varphi1}, \quad \varepsilon_2 = w_1^2 u'_{21} + \varepsilon_1 u_{21}, \qquad (14)$$

where w_1 and ε_1 are the given angular velocity and acceleration of crank 1.

Displacement l_{AD3} of point D_3 belonging to slider 3 and locating at the beginning of its threaded part, is determined as $l_{AD3} = (l_{AC} + l_{CD3})$, where l_{AC} is the length that is determined from (6), l_{CD3} is the constant length that is constructively given. Angle φ_4, which determines the rotation of nut 4 relative to slider 3, is determined as:

$$\varphi_4 = \frac{2\pi \cdot \Delta l_{AD3}}{(p_1 + p_2)}, \qquad (15)$$

where Δl_{AD3} is the displacement change of slider 3, p_1 is the pitch between the screw part of slider 3 and nut 4, p_2 is the pitch between nut 4 and the screw part of fixed link 5.

Displacement l_{AD4} of point D_4, belonging to nut 4 and locating at its center, is determined as:

$$l_{AD4} = l_{AD3} + l_{34}, \qquad (16)$$

where l_{34} is the variable length that determines the displacement of nut 4 relative to slider 3, $l_{34} = l_{34}^0 + l_{34}^1$, where l_{34}^0 is the constant length that indicates initial displacement of nut 4 relative to slider 3, l_{34}^1 is the displacement of nut 4 per its rotation, $l_{34}^1 = \varphi_4 p_1/2\pi$ or $l_{34}^1 = \Delta l_{AD3}p_1/(p_1 + p_2)$.

Due to the screw movement of nut 4, it has velocities and accelerations in two planes: linear (V_4^L, a_4^L) in plane yOz and radial (V_4^R, a_4^R) in plane xOz, where angular components (w_4, ε_4) also appear. These parameters are determined from the following expressions:

$$V_4^L = V_C\frac{p_2}{(p_1+p_2)}, \ a_4^L = a_C\frac{p_2}{(p_1+p_2)}, \ w_4 = \frac{2\pi \cdot V_C}{(p_1+p_2)}, \ \varepsilon_4 = \frac{2\pi \cdot a_C}{(p_1+p_2)}, \ V_4^R = w_4 d_4/2,$$
$$a_4^R = \varepsilon_4 d_4/2, \qquad (17)$$

where d_4 is the diameter of nut 4.

4. Results and Discussion

To determine the numerical values of variable parameters, accept the following values of the constant parameters: rotation speed of crank 1, n_1 = 5 rpm at constant angular velocity (w_1 = const); the length of crank 1, l_1 = 0.07 m; the length of connecting rod 2, l_2 = 0.135 m; the length of the screw-free part CD_3 of slider 3, l_{CD3} = 0.25 m; constant length l_{34}^0 = 0.025 m; the diameter of nut 4, d_4 = 0.024 m.

It becomes possible to obtain the motion trajectories of the end-effector (nut 4) that differ in curvature and twisting when setting different values of screw pitches p_1 and p_2, while having unchanged slider-crank part of the mechanism. Address to calculate the numerical values of the variable parameters of the end-effector (V_4^L, a_4^L, φ_4, w_4, ε_4, l_{34}, l_{AD4}) considering different values of pitches p_1 and p_2. Parameters V_4^R and a_4^R change in proportion to parameters w_4 and ε_4. Therefore, the determination of the functions of parameters V_4^R and a_4^R can be neglected. Discuss three cases of screw pitches combination:

1. When $p_1 = p_2$, particularly {p_1 = 5 mm, p_2 = 5 mm}.
2. When $p_1 < p_2$, particularly {p_1 = 5 mm, p_2 = 10 mm}, {p_1 = 8 mm, p_2 = 14 mm}, {p_1 = 10 mm, p_2 = 20 mm}, {p_1 = 10 mm, p_2 = 30 mm}, {p_1 = 25 mm, p_2 = 30 mm}.
3. When $p_1 > p_2$, particularly {p_1 = 10 mm, p_2 = 5 mm}, {p_1 = 14 mm, p_2 = 8 mm}, {p_1 = 20 mm, p_2 = 10 mm}, {p_1 = 30 mm, p_2 = 10 mm}.

Figures 3–5 show the diagrams providing the variation of angular parameters of nut 4 (φ_4, w_4 and ε_4) depending on the rotational angle of crank 1 (φ_1). It follows from Figures 3–5 that the angular parameters have the maximal values at screw pitches p_1 = 5 mm, p_2 = 5 mm, while their minimal values are realized at screw pitches p_1 = 25 mm, p_2 = 30 mm. The identical angular parameters are realized at the following screw pitches: {p_1 = 5 mm, p_2 = 10 mm} and {p_1 = 10 mm, p_2 = 5 mm}; {p_1 = 8 mm, p_2 = 14 mm} and {p_1 = 14 mm, p_2 = 8 mm}; {p_1 = 10 mm, p_2 = 20 mm} and {p_1 = 20 mm, p_2 = 10 mm}; {p_1 = 10 mm, p_2 = 30 mm} and {p_1 = 30 mm, p_2 = 10 mm}. This is due to the fact that nut 4 moves over the identical path along a helical trajectory for the same time period. The maximal value of the rotational angle of nut 4 (φ_4) is realized at φ_1 = 180° for all diagrams shown in Figure 3.
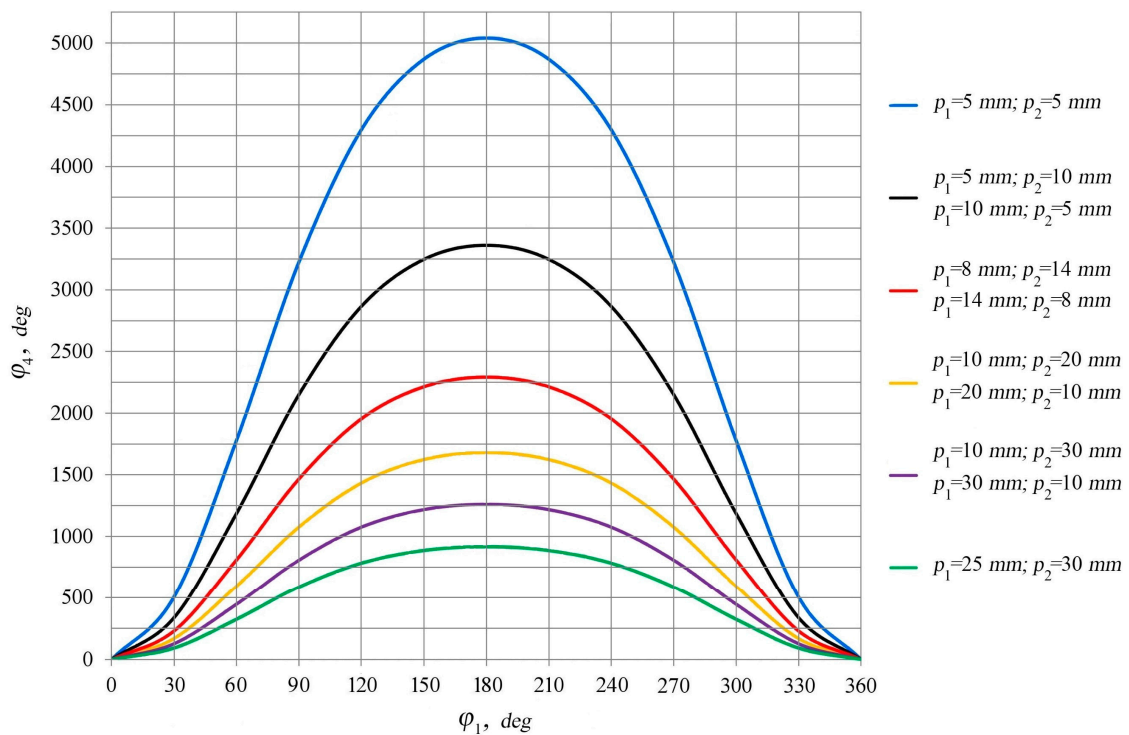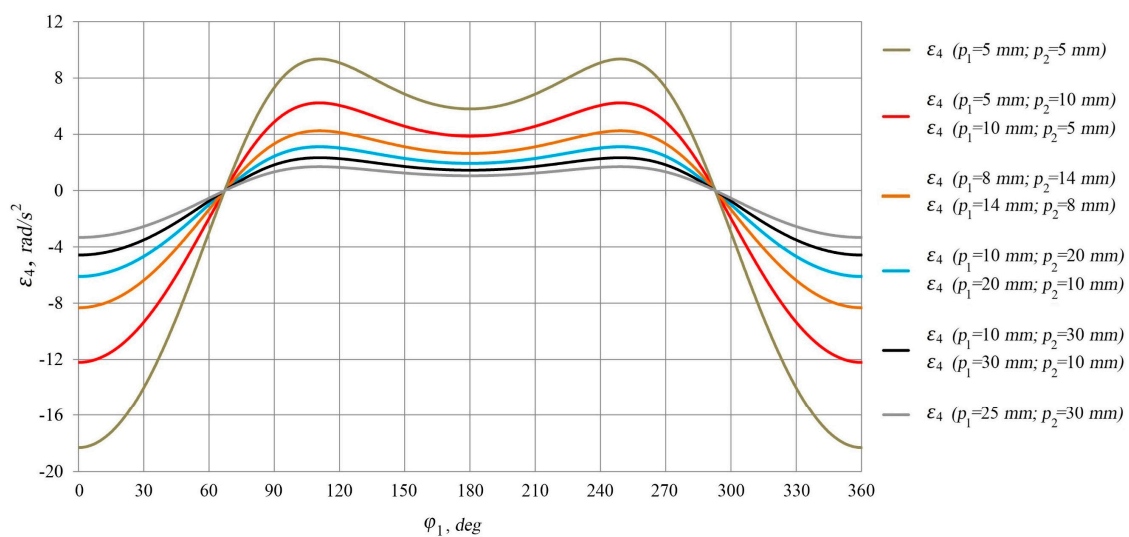

Figure 3. Dependency diagrams of the rotational angle (φ_4) of the end-effector (nut 4) at different pitches (p_1 and p_2) in screw kinematic pairs 3–4 and 4–5.

Figures 6 and 7 show the diagrams providing the variation of linear velocities (V_4^L) and accelerations (a_4^L) of nut 4 depending on the rotational angle of crank 1 (φ_1). The maximal linear velocity is realized at screw pitches p_1 = 10 mm, p_2 = 30 mm, and the minimal linear velocity is at screw pitches p_1 = 30 mm, p_2 = 10 mm. Conversely, the maximal linear acceleration is realized at screw pitches p_1 = 30 mm, p_2 = 10 mm, and the minimal acceleration is at screw pitches p_1 = 10 mm, p_2 = 30 mm. The identical linear velocities and accelerations of nut 4 are realized at the following screw pitches: {p_1 = 5 mm, p_2 = 10 mm} and {p_1 = 10 mm, p_2 = 20 mm}; {p_1 = 10 mm, p_2 = 5 mm} and {p_1 = 20 mm, p_2 = 10 mm}. This is due to the identical functions $l_{34}(\varphi_1)$ and $l_{AD4}(\varphi_1)$, which determine the displacement of nut 4.
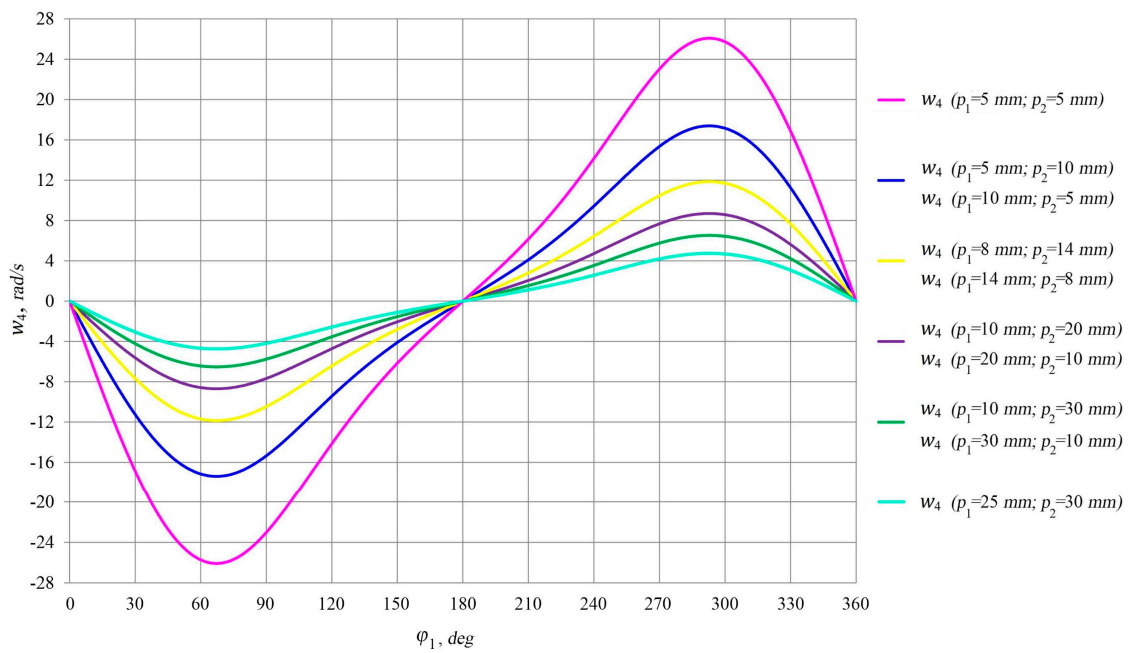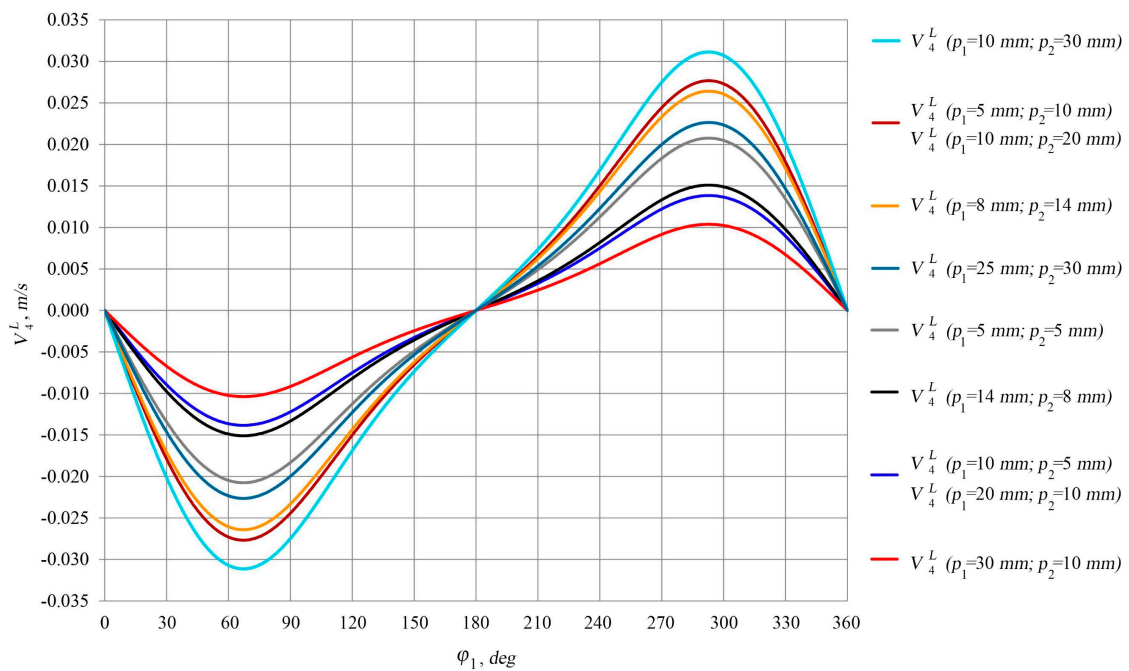
Figure 4. Dependency diagrams of the angular velocity (w_4) of the end-effector (nut 4) at different pitches (p_1 and p_2) in screw kinematic pairs 3–4 and 4–5.
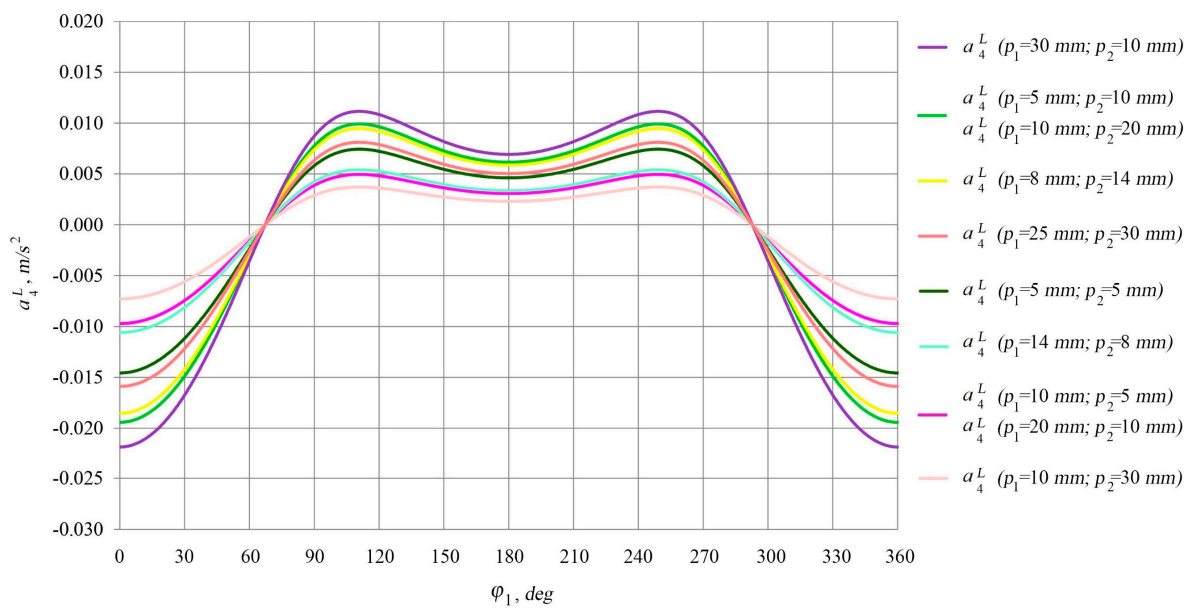

Figure 5. Dependency diagrams of the angular accelerations (ε_4) of the end-effector (nut 4) at different pitches (p_1 and p_2) in screw kinematic pairs 3–4 and 4–5.

It follows from Figures 4 and 6 that the maximal values of the angular and linear velocities (w_4, V_4^L) of nut 4 are realized at $\varphi_1 = 67.2°$ and $\varphi_1 = 292.8°$ at zero accelerations ($\varepsilon_4 = 0$, $a_4^L = 0$). From Figures 5 and 7, it follows that the maximal angular and linear accelerations (ε_4, a_4^L) of nut 4 are realized at $\varphi_1 = 0°$ and $\varphi_1 = 360°$ at zero velocities ($w_4 = 0$, $V_4^L = 0$).

Figure 8 provides the displacement diagram of slider 3 relative to fixed link 5 (l_{AD3}) and the displacement diagrams of nut 4 relative to fixed link 5 (l_{AD4}) depending on the rotational angle of crank 1 (φ_1). The maximal value of l_{AD4} is realized at $\varphi_1 = 0°$ and $\varphi_1 = 360°$ for all diagrams. Figure 8 also provides the displacement of nut 4 relative to slider 3 (l_{34}), determined by the distance from the lower diagram (l_{AD3}) to the corresponding upper diagram (l_{AD4}). The maximal value of l_{34} is at $\varphi_1 = 180°$ for all diagrams, and the largest value of l_{34} is when screw pitches $p_1 = 30$ mm, $p_2 = 10$ mm.
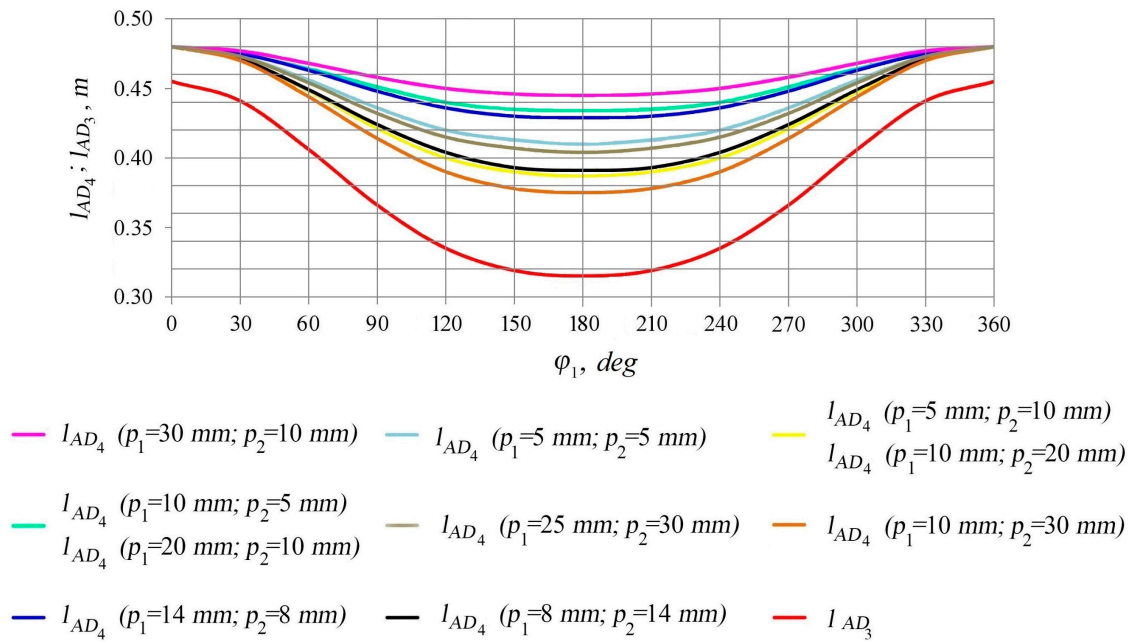
Figure 6. Dependency diagrams of the linear velocities (V_4^L) of the end-effector (nut 4) at different pitches (p_1 and p_2) in screw kinematic pairs 3–4 and 4–5.


Figure 7. Dependency diagrams of the linear accelerations (a_4^L) of the end-effector (nut 4) at different pitches (p_1 and p_2) in screw kinematic pairs 3–4 and 4–5.

Figure 8. Displacement diagrams of slider 3 (l_{AD3}) and end-effector-nut 4 (l_{AD4}) relative to fixed link 5 at different pitches (p_1 and p_2) in screw kinematic pairs 3–4 and 4–5.

Numerical calculations have been carried out to verify the obtained analytical results. The CAD model of the synthesized linkage mechanism has been developed (Figure 9) for this purpose. This model allows to simulate the trajectories of end-effector (nut 4) at different screw pitches p_1 and p_2. The obtained trajectories are presented in Figure 10. Each trajectory is a helix, where the length along axis y is simultaneously determined by both parameters p_1 and p_2, and the pitch of the trajectory is determined exclusively by parameter p_2. The results of the numerical calculation have completely confirmed the obtained analytical data.
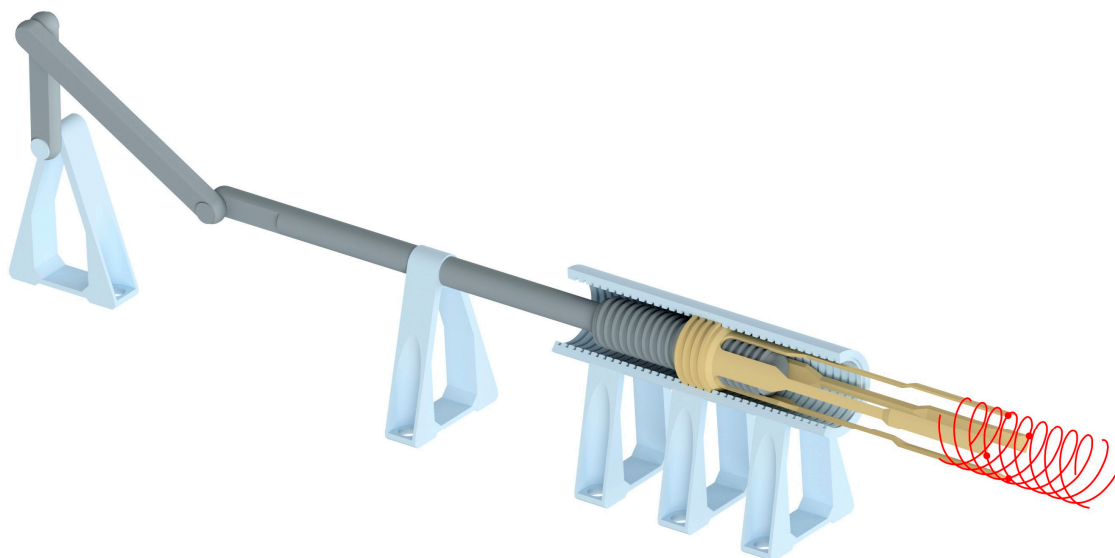
Figure 9. Preliminary CAD model of the synthesized linkage mechanism, designed for the simulation of the motion trajectories of the end-effector.
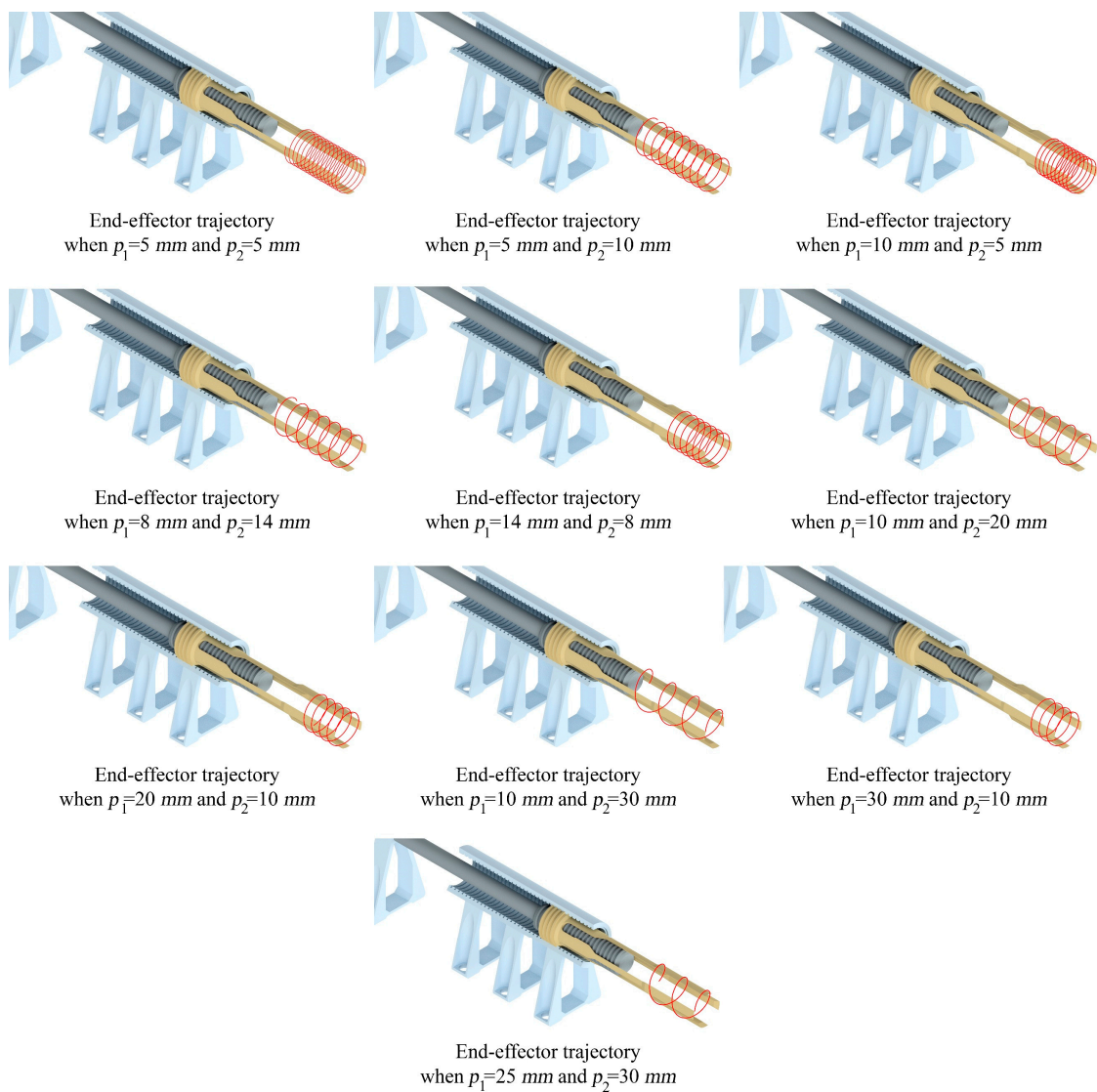
Figure 10. Simulation of the motion trajectories of the end-effector (nut 4) at different pitches (p_1 and p_2) in screw kinematic pairs 3–4 and 4–5.

The motion trajectories presented in Figure 10 clearly demonstrate the effect of screw pitches in helical kinematic pairs 3–4 and 4–5 on the nature of end-effector's movement. The possibility of combining the screw pitches in both pairs allows taking into account additional parameters of the end-effector's trajectories for a given technological operation.

## 5. Development of an Assembling CAD Model and a Physical Prototype of the Mechanism

The detailed assembling CAD model of the synthesized mechanism has been created based on its kinematic scheme. The creation of the CAD model aims a fabrication of an actuated physical prototype on its basis. Figure 11 presents this model, including the following elements: 1–4 are horizontally located elements of the fixed link; 5–8 are vertically located elements of the fixed link for setting motor 13, elements of crank 14 and 15 and slider 17; 9 and 10 are vertically arranged elements of the fixed link for setting elements 11 and 12, which are made with internal thread; 16 is connecting rod; 18 is screw; 19 is nut (end-effector). The dimensions of the CAD model fit with the dimensions of the mechanism indicated in Section 4 when $p_1 = 25$ mm, $p_2 = 30$ mm.
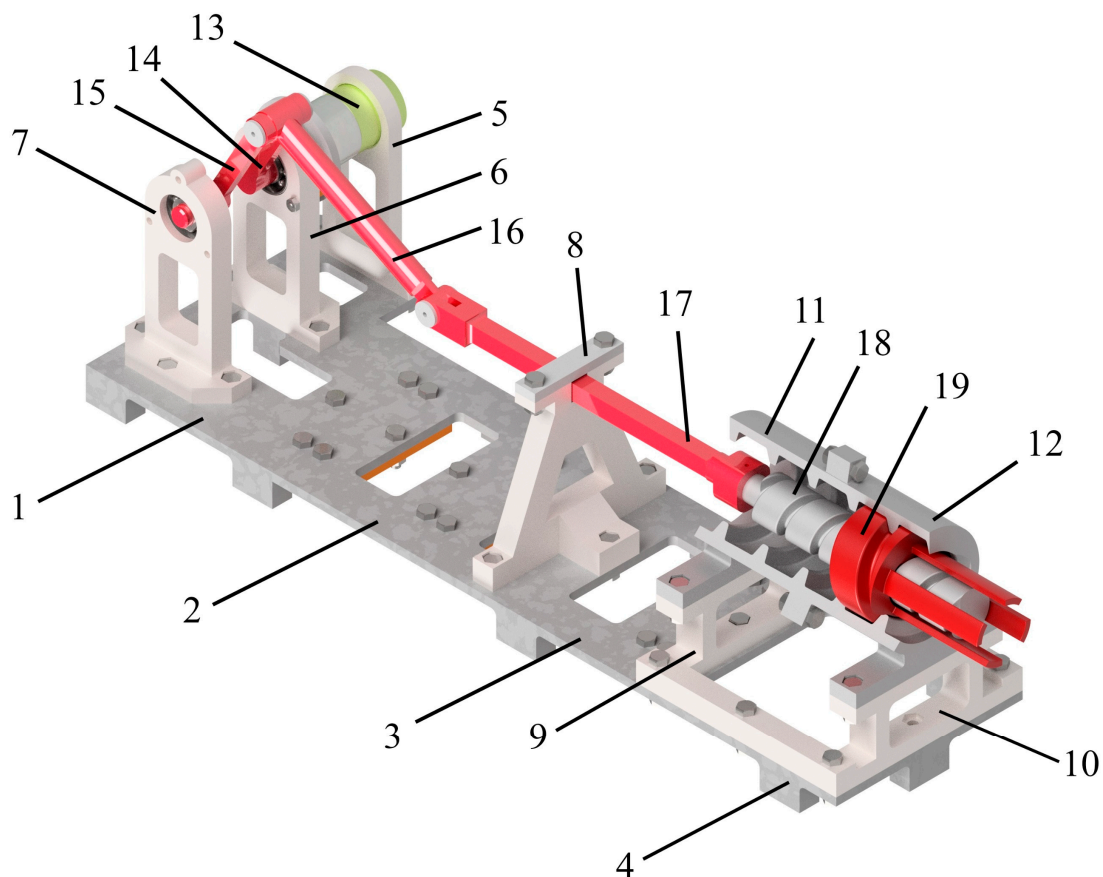
Figure 11. Assembling CAD model of the synthesized linkage mechanism, developed for the fabrication of a physical prototype: 1–12 are elements of the fixed link; 13 is the motor; 14 and 15 are elements of the crank; 16 is the connecting rod; 17 is the slider; 18 is the screw; 19 is the nut (end-effector).

The actuated physical prototype of the synthesized mechanism has been fabricated based on the assembling CAD model shown in Figure 11. Figure 12a presents the manufactured elements of the double screw joint—the screw, nut (end-effector) and screw part of the fixed link. This joint is the most important coupling in the mechanism, its inaccurate manufacture can lead to links jamming and a loss of functionality of the mechanism. Figure 12b shows the full-scale prototype, fabricated in accordance with elements 1–19 of the assembling CAD model. The operation of the physical prototype is presented in the movie in Supplementary Materials. The drive for the prototype has been chosen based on the calculation of the counterbalance moment on the driving link. Such a calculation has been carried out with consideration to reactions and friction forces acting in all kinematic pairs of the mechanism. With respect to threads in the screw joints, multi-turn threads could also be used to reduce forces in these joints and provide a higher load capacity of the end-effector. However, the assembled physical prototype smoothly operates with a single-turn thread.

A comparative analysis of the displacements of certain points of movable links of the CAD model (Figure 11) and the physical prototype (Figure 12) has been carried out to evaluate the accuracy of manufacturing the prototype. The displacements l_{AD3} of point D_3 belonging to slider 3 and the displacements l_{AD4} of point D_4 belonging to nut 4 (end-effector) have been studied. Table 1 presents the numerical values of these parameters in twelve positions of the mechanism. Table 2 summarizes the data on the divergence between the displacements of slider 3 (Δ_1) and nut 4 (Δ_2) of the CAD model and the physical prototype.
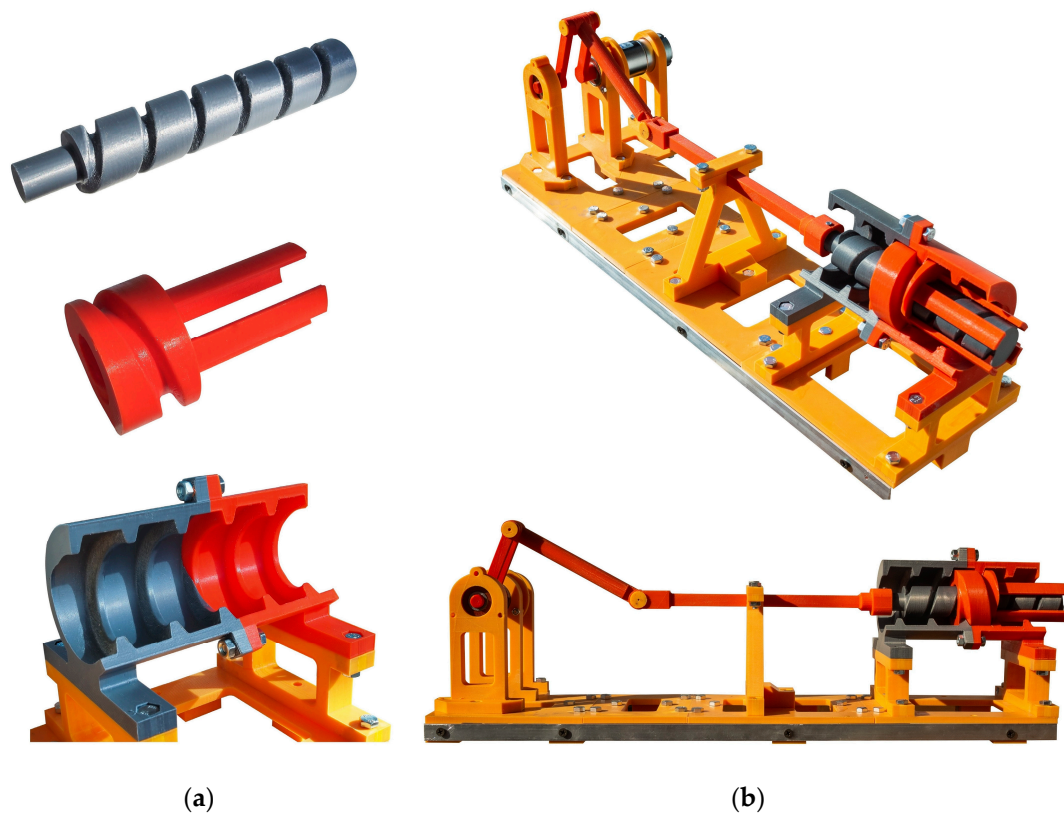
Figure 12. Actuated physical prototype of the synthesized linkage mechanism: (**a**) links of the double screw joint—the screw, nut (end-effector) and screw part of the fixed link; (**b**) full-scale prototype.

Table 1. Numerical values of the displacements of slider 3 (l_{AD3}) and end-effector–nut 4 (l_{AD4}) for the CAD model and the physical prototype of the mechanism in twelve positions.

|		Driving Link Rotational Angle φ_1, *deg*											
		30	60	90	120	150	180	210	240	270	300	330	360
CAD model	l_{AD3}, m	0.441	0.406	0.366	0.335	0.319	0.315	0.319	0.335	0.366	0.406	0.441	0.455
	l_{AD4}, m	0.473	0.454	0.432	0.415	0.407	0.404	0.407	0.415	0.432	0.454	0.473	0.480
Physical prototype	l_{AD3}, m	0.444	0.408	0.368	0.337	0.321	0.316	0.321	0.337	0.368	0.409	0.444	458.0
	l_{AD4}, m	0.477	0.458	0.435	0.418	0.410	0.406	0.409	0.417	0.433	0.457	0.478	0.484

Table 2. Calculation of the divergences between the displacements of slider 3 (Δ_1) and end-effector–nut 4 (Δ_2) for the CAD model and the physical prototype of the mechanism in twelve positions.

	Driving Link Rotational Angle φ_1, *deg*											
	30	60	90	120	150	180	210	240	270	300	330	360
Δ_1, %	0.68	0.49	0.55	0.60	0.63	0.32	0.63	0.60	0.55	0.74	0.68	0.66
Δ_2, %	0.85	0.88	0.69	0.72	0.74	0.50	0.49	0.48	0.23	0.66	0.63	0.83

It follows from Table 2 that the maximal value of Δ_1 is 0.74% at $\varphi_1 = 300°$, and the maximal value of Δ_2 is 0.88% at $\varphi_1 = 60°$. The occurrence of divergences Δ_1 and Δ_2 is associated with inaccuracies during the manufacture of mechanism elements by means of three-dimensional printing from polymeric materials. However, achieving divergences of Δ_1 and Δ_2 less than 1% is thoroughly acceptable, taking into account the complexity of the double screw kinematic pair and fabrication of mechanism elements from polymeric materials.

6. Possibilities of Technological Application of the Mechanism

The possibilities of the practical application of the synthesized mechanism have been considered in this study. Virtual models for performing specific technological operations have been developed based on the mechanism's kinematic scheme. Specifically, the mechanism can be used for large-diameter springs' winding. Figure 13a shows a virtual model where a spring is wound onto a mandrel that simultaneously becomes displaced and rotates at predetermined distances and angles. Here, the wire is moved through the rollers mounted on the fixed link, and the end of the wire is fixed on the mandrel, which is rigidly connected to the end-effector of the mechanism. The velocity of the mandrel is controlled by the driving link of the mechanism and is in the range of 10–40 m/min depending on the diameter of the wire. After the driving link moves to the end position, the winding process ends and the spring is removed. After that, the driving link makes the remaining half of a revolution and the mandrel is shifted to its initial position to perform the next operation.

(**a**)

(**b**)
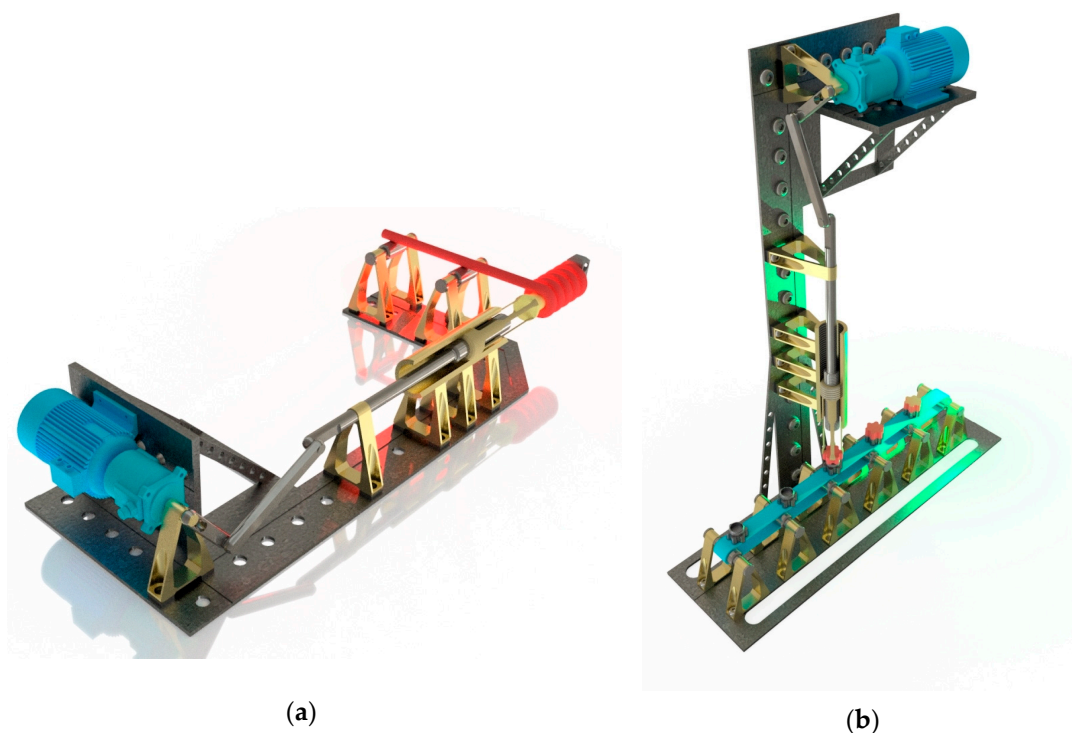
Figure 13. Virtual models of technological units with the application of the synthesized mechanism: (**a**) for spring winding; (**b**) for screwing various objects.

The helicoidal motion of the end-effector of the synthesized mechanism allows using it to screw various objects [17]. A virtual model of such a technological unit is shown in Figure 13b, where the developed mechanism is located vertically. It allows screwing objects moving under the end-effector on which the gripper is set. The linear displacement and rotation of the gripper are determined by the kinematic parameters of the mechanism. The screwing is realized in a time equal to half of the driving link rotation. During the second half of the driving link rotation, the next object is placed under the gripper and the operation is repeated.

The practical application of the synthesized mechanism is not limited to the proposed technological units shown in Figure 13. The mechanism can also be implemented for other operations that require the cyclic movement of the end-effector along a helical path. Such operations may also include mixing processes, cleaning inner cylindrical surfaces, etc.

7. Conclusions

This study presents a novel one-DoF mechanism formed by the sequential coupling of planar and helical kinematic chains. The developed mechanism is synthesized with a minimum number of links and joints, while its end-effector, forming two screw joints at the same time, performs a cyclic motion along a helicoidal trajectory. The design of the mechanism is made in such a way that all its links, except the end-effector, have planar motions. This ensures minimal dynamic forces in those directions where the movements of links are restricted. The study provides an analytical solution of kinematic analysis; specifically, the problems of positions, velocities and accelerations have been solved. The analytical kinematics algorithm has been verified by numerical calculations. In addition, the modeling of spatial trajectories of the end-effector at different pitches of the screw joints has been carried out. A detailed assembling CAD model of the mechanism has been designed, on the basis of which an actuated physical prototype has been fabricated. A functional performance of the prototype has been analyzed by comparing the displacements of its end-effector with analogical displacements of the assembling CAD model. The question of possible technological applications of the synthesized mechanism has been considered in this study. In this regard, virtual models of engineering units for spring winding and various objects screwing have been developed.

References

1. Crossley, F.R.E. The permutation of kinematic chains of eight members or less from the graph-theoretic viewpoint. *Dev. Theor. Appl. Mech.* **1965**, *2*, 467–486.
2. Schmidt, L.C.; Shetty, H.; Chase, S.C. A graph grammar approach for structure synthesis of mechanisms. *ASME J. Mech. Des.* **2000**, *122*, 371–376. [CrossRef]
3. Fomin, A.; Paramonov, M. Synthesis of the four-bar double-constraint mechanisms by the application of the Grubler's method. *Procedia Eng.* **2016**, *150*, 871–877. [CrossRef]
4. Kong, X.; Gosselin, C.M. Type Synthesis of Single-Loop Kinematic Chains. In *Type Synthesis of Parallel Mechanisms*, 1st ed.; Springer: Berlin/Heidelberg, Germany, 2007; p. 276.
5. Glazunov, V. Design of decoupled parallel manipulators by means of the theory of screws. *Mech. Mach. Theory* **2010**, *45*, 239–250. [CrossRef]
6. Dvornikov, L.T. Experience of structural synthesis of mechanisms. *Theory Mech. Mach.* **2004**, *2*, 3–17.
7. Gogu, G. Mobility of mechanisms: A critical review. *Mech. Mach. Theory* **2005**, *40*, 1068–1097. [CrossRef]
8. Li, S.; Wang, H.; Dai, J.S. Assur-group inferred structural synthesis for planar mechanisms. *ASME J. Mech. Robot.* **2015**, *7*, 041001. [CrossRef]
9. Peisakh, E.E. Structural analysis of planar jointed mechanisms: Current state and problems. *J. Mach. Manuf. Reliab.* **2008**, *37*, 207–212. [CrossRef]
10. Campos, A.; Budde, C.; Hesselbach, J. A type synthesis method for hybrid robot structures. *Mech. Mach. Theory* **2008**, *43*, 984–995. [CrossRef]
11. Zhang, X.; Zhang, X. A comparative study of planar 3-RRR and 4-RRR mechanisms with joint clearances. *Robot. Cim. Int. Manuf.* **2016**, *40*, 24–33. [CrossRef]
12. Lee, C.C.; Herve, J.M. A blend of Delassus four-bar linkages. In *Computational Kinematics. Mechanisms and Machine Science*; Thomas, F., Perez Gracia, A., Eds.; Springer: Dordrecht, The Netherlands, 2014; Volume 15.
13. Huynh, P.; Herve, J.M. Equivalent kinematic chains of three degree-of-freedom tripod mechanisms with planar-spherical bonds. *J. Mech. Des.* **2005**, *127*, 95–102. [CrossRef]

14. Jones, M.H.; Velinsky, S.A. Kinematics of roller migration in the planetary roller screw mechanism. *J. Mech. Des.* **2012**, *134*, 061006. [CrossRef]

15. Wei, C.C.; Lin, J.F. Kinematic analysis of the ball screw mechanism considering variable contact angles and elastic deformations. *J. Mech. Des.* **2004**, *125*, 717–733. [CrossRef]

16. Fomin, A.; Ivanov, W. Development of a mixing mechanism with a complex motion of the end-effector. *Stroj. Vestn. J. Mech. E* **2019**, *65*, 319–325. [CrossRef]

17. Yang, H.; Liu, X.; Xu, G.; Xu, Z.; Ma, J. Design of eccentric bunghole cap screwing-pressing machine based on robot vision technique. In Proceedings of the IEEE Advanced Information Technology, Electronic and Automation Control Conference (IAEAC), Chongqing, China, 19–20 December 2015; pp. 465–469.